Osteoarthritis Alters the Patellar Bones Subchondral Trabecular Architecture

Sebastian Hoechel,[1] Hans Deyhle,[2] Mireille Toranelli,[1] Magdalena Müller-Gerbl[1]

[1]Department of Biomedicine, Musculoskeletal Research, University of Basel, Pestalozzistrasse 20, 4056 Basel, Switzerland, [2]Biomaterials Science Center, University of Basel, Gewerbestrasse 14, 4123 Allschwil, Switzerland

Received 25 November 2015; accepted 11 November 2016
Published online in Wiley Online Library (wileyonlinelibrary.com). DOI 10.1002/jor.23490

ABSTRACT: Following the principles of "morphology reveals biomechanics," the cartilage-osseous interface and the trabecular network show defined adaptation in response to physiological loading. In the case of a compromised relationship, the ability to support the load diminishes and the onset of osteoarthritis (OA) may arise. To describe and quantify the changes within the subchondral bone plate (SBP) and trabecular architecture, 10 human OA patellae were investigated by CT and micro-CT. The results are presented in comparison to a previously published dataset of 10 non-OA patellae which were evaluated in the same manner. The analyzed OA samples showed no distinctive mineralization pattern in regards to the physiological biomechanics, but a highly irregular disseminated distribution. In addition, no regularity in bone distribution and architecture across the trabecular network was found. We observed a decrease of material as the bone volume and trabecular thickness/number were significantly reduced. In comparison to non-OA samples, greatest differences for all parameters were found within the first mm of trabecular bone. The differences decreased toward the fifth mm in a logarithmic manner. The interpretation of the logarithmic relation leads to the conclusion that the main impact of OA on bony structures is located beneath the SBP and lessens with depth. In addition to the clear difference in material with approximately 12% less bone volume in the first mm in OA patellae, the architectural arrangement is more rod-like and isotropic, accounting for an architectural decrease in stability and support. © 2016 Orthopaedic Research Society. Published by Wiley Periodicals, Inc. J Orthop Res

Keywords: osteoarthritic trabecular changes; human patella; subchondral bone plate mineralization; 3D micro-CT

Bone, as dynamic tissue, constantly balances its formation and resorption process to maintain an optimal supportive structure and meet the mechanical demands. In accordance to the biomechanics of a joint and the resulting pressure distribution, these adaptational processes can be seen in the distribution pattern of the thickness and mineral distribution of the subchondral bone plate (SBP).[1–7] Following these principles of "morphology reveals biomechanics," the mineral distribution of the SBP and the architecture of the trabecular just beneath show similar morphologic characteristics. Maxima of mineral embedment are regularly found in the more heavily loaded areas within the SBP of a joint surface. Therefore, such maxima are found on the talar edges, decreasing toward the center of the medial groove,[8] on the medial condyle of the tibial plateau in comparison to the lateral,[3] and on the lateral patellar facet.[9] The latter one is due to the greater contact force applied to the lateral facet through the displacement vector of the quadriceps muscle (quadriceps angle).

The dynamics of these density patterns in regards to changes of the biomechanics following pathological conditions were shown in an animal meniscectomy model where the maxima of mineralization shifted following the altered mechanical situation.[10] Studies on patients following tibial osteotomy for genu varum also revealed a shift of maxima location after successful realignment. One year postoperative, peak mineralization on the medial condyle centralized, and the lateral condyle showed increased calcium hydroxyapatite deposition, corresponding to the theoretical expectations.[6] Since the SBP links to the cancellous bone beneath, the absorbed load is forwarded into the trabecular system. Here, the trabecular bone adapts to the mechanical environment as a function of the pressure which is put forward.[11] Following the applied theorems of stereology on 2D sections of early investigations, direct three-dimensional (3D) measurements have emerged. Now it is possible to determine the microarchitecture of trabecular bone in a direct manner, saving the time consuming sectioning process and the inaccuracy of assumptions.[12–14] In addition to the common differences in trabecular architecture as function of anatomic position, loading direction, and load accumulation over time,[15,16] precise correlations to individual long-term load intake are described.[17,18]

In case of a compromised relationship between the loading in a joint and the ability of its components to support the load, the pathogenesis of osteoarthritis (OA) as a disease of the whole joint may arise.[19–21] Next to typical cartilage lesions, changes within the subchondral bone seem to play an important role in the dynamics of the disease. Whether the cartilage lesions are the trigger factor or a secondary consequence of the subchondral bone changes is still debated.[22] Nevertheless, models of induced OA lead to subchondral bone changes with subsequent trabecular remodeling resulting in a less compliant trabecular bone, and therefore, excessive stress in the overlying articular cartilage.[23,24]

Conflicts of interest: None.
Grant sponsor: Swiss National Science Foundation; Grant number: 316030_133802/1.
Correspondence to: Sebastian Hoechel, (T: +41 (0) 61 267 39 37; F: +41 (0) 61 267 39 59; E-mail: sebastian.hoechel@unibas.ch)

As one of the most severe causes of knee pain in the elderly population, patellofemoral OA changes lead to anterior knee pain causing difficulties in daily routine including gait, stairs, and squatting.[25,26] The resulting impairments of function as well as the pain are thought to be the consequence of trauma or changes within the pressure distribution of the patellofemoral joint particularly following meniscal tear or rupture of the cruciate ligaments.[27,28]

As for the patella, the literature describes cartilage lesions more severe than Outerbridge Grade II in more than 63% in the elderly population. Here, the depth of the lesion correlates to the anterior knee pain. Also, it has been shown that females are more affected by cartilage lesions than males.[29]

The architectural changes within the subchondral bone of the patella can until now only be assumed using the existing concepts of OA, where non-physiological strain initiates a cascade reaction of bone alteration.

In this case, the early onset of cartilage degeneration is accompanied by a sclerosis of the SBP and an increase in trabecular thickness and density. It leads to a progressive change of trabeculae form rodlike to platelike, the opposite of the processes in normal aging.[30] Late-stage OA (according to the Kellgren and Lawrence radiographic criteria: grade 4) on the other hand, shows a decrease of bone mineral density.[31]

To further evaluate this effect of late stage OA and describe the changes occurring in the trabecular architecture, this study analyses directly derived 3D-micro-CT data models, to gain information of architectural trabecular parameters as a function of localization.

We therefore, aim to describe the regional distribution of bone parameters and their correlation to the individual long-term load intake via:

(1) The description of the mineralization and the thickness of the SBP in late-stage OA patellae as markers of the long-term load intake;
(2) The evaluation of the trabecular architecture of late-stage OA patellae
    a. Beneath the entire SBP to achieve demonstration of the regional distribution
    b. In 1 mm steps (layers), starting just beneath the SBP to a depth of 5 mm to describe the development of OA into depth.

Since the anatomy of the SBP and trabecular network of 10 non-OA patellae of the elderly population has already been described we intent to:

(3) Compare the findings to a previously published dataset of non-OA samples which were in the same age group and analyzed using the same methods to directly draw conclusions on the late-stage OA changes of the trabecular network.

MATERIALS AND METHODS

Materials

Ten formalin-fixed, OA human patellae were used (five male, five female; age 60–74 years, mean 69.4; unknown medical history). The inclusion criteria was specified as cartilage degeneration of Outerbridge IV on the medial and/or lateral facets.

In consideration of The Code of Ethics of the World Medical Association (Declaration of Helsinki), for experiments involving humans, the samples were taken from body-donors to the Department of Anatomy, University of Basel, who contributed their body to science and research only.

Methods

Density Distribution of the Subchondral Bone Plate

Using conventional CT-datasets (SOMATOM 16, Siemens, Erlangen, Germany, 120 kilovolt [kV], 180 milliampere-second [mAs], slice thickness 0.6 mm, axial slices) of the samples, we evaluated the density distribution of the SBP with the help of the software ANALYZE® 11.0 (Biomedical Imaging Resource, Mayo Foundation, Rochester, MN). According to the mineral content, the "maximum intensity projection-algorithm" projects the densest voxel within the SBP onto the surface in a color-coded manner. Starting with Hounsfield units (HU) greater than 1,200 in black, the colors descended in steps of 200 HU to red, yellow, green, and blue.[6,17,32]

The CT-osteoabsorptiometry method has been evaluated using dual-energy quantitative computed tomography and validated in comparison to the analysis of fresh and frozen samples (discrepancy of 0.5%).[6] Therefore, the density distribution with respect to the HU directly links to the calcium hydroxyapatite concentration, which was calculated.

Micro-CT Measurements

Micro-CT experiments were performed with the General Electric phoenix nanotom® m system (Wunstorf, Germany) with an acceleration voltage of 140 kV, beam current of 60 μA, and a 0.1 mm aluminum-filter to reduce beam-hardening. The patella was placed in a polyethylene container filled with fixation solution to prevent the tissue from drying. The 2,100 projections (exposure time: 0.5 s) were recorded over 360 degrees, defining the resulting isotropic pixel size of 32 μm. Reconstruction was performed with the datosx software (GE, Wunsdorf, Germany) based on a modified Feldkamp algorithm.[33]

In accordance to a previously conducted study on non-OA patellae, the 3D datasets of the patellae were divided into 21 measuring cubes ($8 \times 8\,mm^2 \times$ SBP to anterior cortical bone) using the visualization and analysis software VGStudio® Max 2.2 (Heidelberg, Germany).[17] All cubes were separately analyzed to present a topographical parameter distribution across the entire articulation surface.

In the first step, the thickness of the SBP was evaluated. Following this evaluation, the trabecular bone of the first 5 mm (1st ROI: 0–1 mm of trabecular bone below the SBP, 2nd ROI: 1–2 mm, likewise for the 3rd, 4th, and 5th ROI) beneath the SBP of the produced measuring cubes were analyzed (Fig. 1) with the help of the Skyscan software CT-analyser® (Bruker-Microct, Kontich, Belgium).[17] All analysis were performed using an automatic surface detection system in accordance to the threshold distribution of the dataset and provide a complete inter-observer independence.

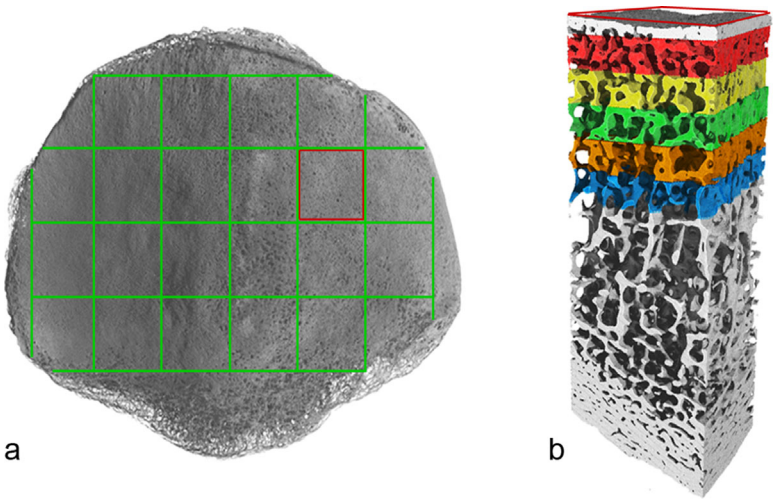

Figure 1. Method of μ-CT; definition of measurement cube and regions of interest. a) 3D reconstruction, left patella in dorsal view, 21 areas for extraction of measurement cubes marked. b) Measurement cube with five highlighted regions of interest (1st ROI: red; 2nd ROI: yellow; 3rd ROI: green; 4th ROI: orange; 5th ROI: blue) just below the subchondral bone plate.

The obtained parameters of bone histomorphometry and architecture were selected according to literature recommendations of bone analysis and are as follows[13,34–36]:

(1) BV/TV, (%); indices of bone volume (BV) in relation to the total volume (TV); a parameter of trabecular bone that is contained within a biphasic region of solid structure and space, it resembles the proportion of the ROI occupied by solid material;
(2) BS/TV, (1/mm); bone surface density (BS) in relation to the TV; this 3D trabecular surface is based on the faceted surface of the binarised ROIs and describes the bone surface per TV in every 1 mm ROI across the whole patellar articular surface;
(3) Tb.Th, (mm); parameter of dimension for the trabecular thickness; truly measured, model-independent parameter that determines an average of the local thickness at each voxel representing bone. It is defined as diameter of a sphere, which encloses the point (not necessarily the center) and is still entirely contained within the solid surfaces; and
(4) Tb.Sp, (mm); trabecular separation; directly and model-independently measured in 3D by the same method used to measure trabecular thickness; as primary measurements in bone histomorphometry.

Derived indices:

(5) Tb.N, (1/mm); the trabecular number; it implies the number of traversals across a trabecular made per unit length on a linear path through a bony region and is measured in 3D by application of an equation for the parallel plate model using direct 3D measurements of Tb.Th and BV/TV; as structural parameter. As well as:
(6) SMI, (dimensionless); the structure model index; indicating the relative prevalence of plate-like or rod-like architecture within the 3D trabecular network. It involves a measurement of the surface convexity and is based on dilation of the 3D voxel model, which is the artificial addition of one voxel thickness to all binarised object surfaces. The SMI values of an ideal plate, cylinder, and sphere model are 0, 3, and 4, respectively; and
(7) DA, (dimensionless); the degree of anisotropy; describing the presence or absence of the alignment of structures preferentially along a particular directional axis. Results of DA range from 0 (total isotropy) to 1 for total anisotropy, that can be described as columns of trabecular without interconnections.

Statistical Analysis

Depth based data analyses were performed for every measuring cube. Afterward, the mean value of all ROIs on the same level for every analyzed parameter was used as result.

The presented data were analyzed for each patella. The results are referenced to the data collected on a non-OA sample population (five male and five female; mean age 72 years, range 65–78 years; six right samples, four left) from a previous study, where the same methods and analysis techniques were used.[17]

Statistical analysis included the Pearson product-moment correlation coefficient, a two-tailed *t*-test stating the significance as well as the Kolmogorov–Smirnov test for evaluation of the distribution level of the data. A p-value of <0.05 was considered as statistically significant. All analyses were performed using RStudio® (RStudio®: Integrated-development environment for R, Version 0.99.467, Boston, MA).

RESULTS

Mineral Distribution of the Subchondral Bone Plate

The mineralization within the SBP of the OA population showed a strong irregularity with multi-located spot like maxima covering the whole articulating surface. Especially in areas where completely detached chondral fragments were present, these maxima were often surrounded by lacunae of low mineralization with differences of up to 400–450 mg/ml. Furthermore, the pathological osteophyte formations around the rim showed a high variation of calcium hydroxyapatite with local peaks of enrichment (Fig. 2b).

In comparison to the non-OA population (Fig. 2a), there were no signs of regularity for the pattern of mineral distribution. The positions of the found maxima and minima were in no relation to a physiological load distribution within the patellofemoral joint. The absolute range of mineralization of the evaluated maxima and minima did not differ significantly

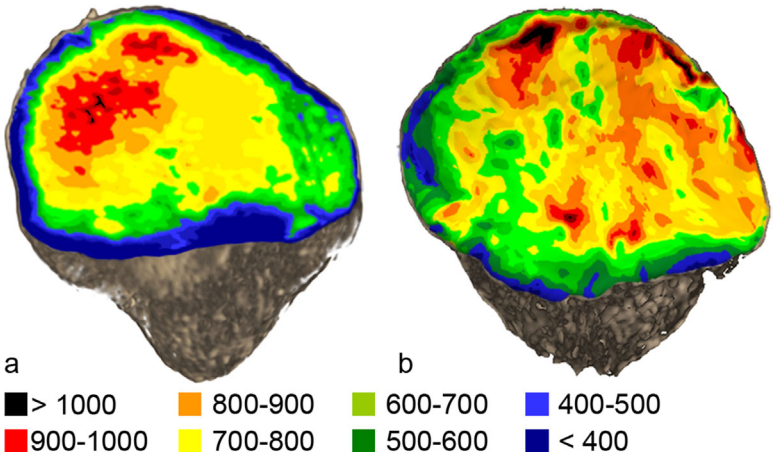

Figure 2. Representative mineralization pattern according to the density distribution of the human patella (mg/ml calcium hydroxyapatite; left = lateral). a) Non-OA patella[17] b) OA patella.

($p = 0.43$) in comparison to the non-OA samples. The peak values of the maxima ranged from 845 to 1,080 mg/ml (non-OA samples: 880–1,047 mg/ml), the lowest measured mineral values ranged from 380 to 420 mg/ml (non-OA samples: 377–437 mg/ml) (Fig. 2a and b).

Micro-CT Measurements

Subchondral Bone Plate Thickness

The SBP of OA patellae presented itself as solid, homogenous build but contained wave-like lamella with a BV/TV of 96–98% (standard deviation (SD) 1.6). Its thickness distribution revealed two maxima with one obvious minimum in between. The maxima were located on the lateral facet (up to 1.25 mm; mean 1.11 mm; SD 0.20 mm) as well as on the medial facet (up to 1.05 mm; mean 0.84 mm; SD 0.25 mm). The minimum of the subchondral bone thickness was situated on the vertical ridge of the patellae, presenting a mean thickness of 0.65 mm (SD 0.35 mm) in its distal parts. The difference between maximum and minimum was statistically significant ($p < 0.05$) (Fig. 3b).

In contrast to the SBP thickness of the OA samples, the non-OA sample population showed only one maximum located on the lateral facet (up to 1.25 mm; mean 1.16 mm; SD 0.25 mm), which gradually decreased toward the periphery including one medial extension with a thickness of 0.65–0.80 mm over the vertical ridge onto the medial facet.

While the SBP of the non-OA samples showed a smooth border in its transition to the calcified cartilage, the OA samples showed a more wave-like appearance extending into an osteophyte formation at its borders to the anterior cortical bone. Comparing the SBP-thickness of both sample collections, no significant difference ($p > 0.05$) was found (Fig. 3a and b).

Trabecular Measurements

The OA population revealed no noticeable distribution pattern of the obtained trabecular measurements within the first 5 mm of analyzed spongy bone. Multiside maxima and minima of all analyzed parameters were present. Still, BV/TV, BS/TV, Tb.Th, and Tb.N showed a steady decrease of absolute value into depth, where the decrease of the absolute parameter value per mm of depth declined with depth showing the largest differences between the first and second mm. This was a steady but declining decrease, and therefore, the development of each of the parameters into

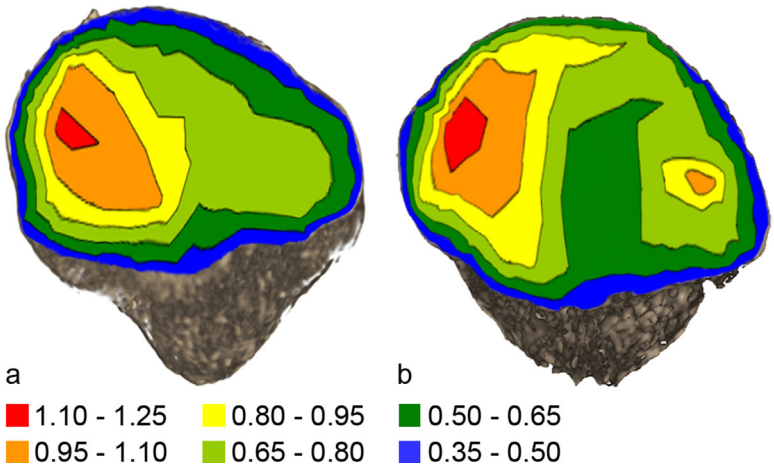

Figure 3. Summation chart of the thickness distribution of the subchondral bone plate (mm; left = lateral). a) Non-OA patellae[17] b) OA patellae.

depth could be described as a logarithmic dependency (Fig. 4). For Tb.Sp, SMI, and DA, an ongoing increase was seen. For these observations, the increase was highest between the first and the second mm and decreased toward the fourth and fifth mm. The dependency of these parameters from depth showed a logarithmic dependency (Fig. 4).

In comparison to the non-OA group, BV/TV, BS/TV, Tb.Th., and Tb.N showed significantly ($p < 0.05$) lower values in the OA group in every analyzed depth in comparison to the non-OA sample collection (Fig. 4). The differences of the absolute value between each layer decreased with depth in the sample, showing the largest absolute differences in the 1st mm, the smallest differences in the 5th mm respect to the absolute value of the non-OA sample reduced in depth.

On the contrary, Tb.Sp, DA, and SMI revealed significantly ($p < 0.05$) higher values in the OA sample population in comparison to the non-OA population (Fig. 4). Here as well, the difference of the absolute parameter value as well as the calculated difference in comparison to the absolute value of the non-OA sample population decreased with depth and revealed the smallest difference in the 5th mm.

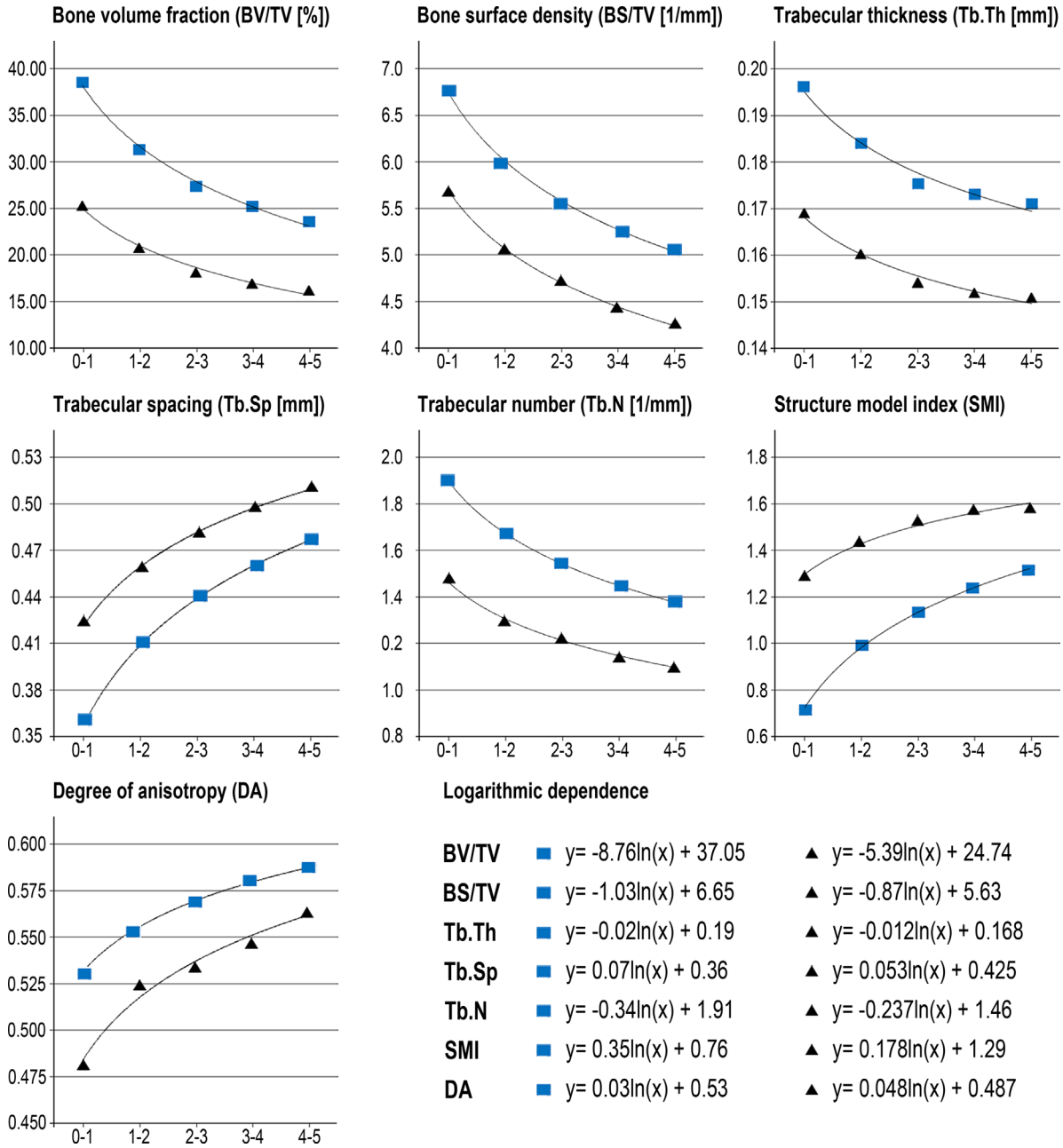

Figure 4. Logarithmic dependency of the architectural parameter development from the first to the fifth millimetre of trabecular bone beneath the subchondral bone plate of the human patella. ■) Non-OA patellae; ▲) OA patellae.

DISCUSSION

In the patella, a chondromalacia or cartilage softening of the lateral facet follows secondary to excessive pressure.[37] On the medial facet, a non-physiological combination of compression and shear stress is described to be the initiating factor.[37] In the end, this loss of elasticity as it is induced by cartilage softening, decreases the functional ability to distribute pressure throughout the articular cartilage, and leads to a mechanical situation where the articular forces are transferred abnormally onto the SBP provoking an adjacent reaction.[37]

Following previous studies of the adaptation of the SBP to pathologically altered long-term load intake, this irregular distribution would result in an abnormal density distribution pattern that can clearly be differentiated from the ones observed in non-OA samples.[9,38,39]

The constant maximum of density and therefore, the deposition of calcium hydroxyapatite on the lateral facet of the patella, as previously described on non-OA samples, was not observed in this study.[6,38] Instead, the deposition was spot-like scattered over the entire joint surface, revealing a long-term load intake that is not in correlation to the applied pressure. In between the spots of high density, lacunae of very low concentration were present.

The mean SBP's thickness distribution over all OA samples represented two maxima, one on the medial and one on the lateral facet. Located on the ridge, we observed a significant minimum. The often-described sclerosis and thickening of the SBP in OA patients can be attributed to the spot-like deposition of calcium hydroxyapatite forming the second maximum on the medial facet as it is not seen in a non-OA study group.[40,41] There, the SBP presented itself significantly ($p < 0.5$) thicker. A significant increase or decrease of the total thickness was not observed. These results do not implicate a more severe change within the medial facet, but a non-physiologic mineralization throughout the SBP of the patella which only than raises the mineralization of the medial side. Nevertheless, on the lateral facet, where the mineral content is higher in general, the now irregular distribution is on the same level as a non-OA hydroxyapatite concentration.

These results are in agreement to previously published data from Eckstein et al. who showed that cartilage lesions lead to a thickening of the SBP in the affected area without exceeding the maximum thickness of non-OA samples.[9] Previously described advancing endochondral ossification and multiplication of the tidemark as well as new bone formation was not seen in this study.[42,43] A partial explanation might be the production of new, un-mineralized, and immature bone formation without the equivalent mineralization, leading to thicker, but less resistant bone that would not be visible during this micro CT analysis.[44]

Since the changes within the cartilage-osseous interface led to alterations of pressure (distribution and) transfer into the trabecular bone system, differences in the 3D network, compared to the non-pathological situation, demonstrate the expected bone turnover associated with OA.

In contrast to studies using bone-cores or cuts from selected areas of OA degenerated bones, we acquired data for the whole trabecular network of pathological patellae for comparison with a non-OA sample collection. Our data allows accessing the trabecular architecture of entire patellae 5 mm in depth under the SBP and is not limited to selected measurements resembling the architectural situation.[45] A comparison of absolute values with those from literature is therefore, difficult, and parallels should only be drawn concerning the statements about the differences of non-OA and OA.

In general, we observed a decrease of material in the OA population, as the BV as well as the trabecular number and thickness decreased, and the trabecular spacing was significantly wider ($p < 0.1$). These results are in agreement with the study by Dedrick et al., who showed a reduced Tb.Th in severe OA, as well as with Ding et al. who also demonstrated a decrease in trabecular bone structure and mechanical properties in OA.[46,47] Recently published results of an anterior cruciate ligament transection model in a rabbit also demonstrated significant reduction of BV/TV and Tb.Th in the medial femoral compartment of the OA knee.[48]

In contrast, analyses of the femorotibial joint published by Kamibayashi et al. and Buckland-Wright et al. showed an increase of BV/TV, due to thick, widely spaced trabecular.[49,50] In regards to the measurement acquisition, one has to note that Kamibayashi et al. used stained histologic sample analysis of 2D images only on the medial tibial plateau and Buckland-Wright et al. used conventional X-ray summation images, which projects the 3D arrangement on a 2D picture, lacking in representation value, and the direct description of the third dimension. Although these methods give insight into the OA of the femorotibial joint, micro CT measurements allow accessing the 3D structure.

Overall, this study substantiates and expands upon the results of Patel et al. published in 2003.[45] They analyzed bone-core specimens from normal and OA knees and described the differences of trabecular parameters for the medial tibial plateau, where they found the most significant differences. They described the BV/TV and Tb.Th to be lower in the OA samples with SMI and Tb.Th being higher, in agreement with our results. Tb.N showed no significant variation, whereas in the patella we observed a significant reduction in the OA sample collection.

Examining the development of the architectural parameters into the depth of the trabecular network we found a logarithmic dependency that showed the greatest difference for all parameters within the first mm, decreasing toward the fifth. This led us to the conclusion that the main impact of OA is beneath the

SBP and lessens with depth. Next to the clear distinction in the amount of material with approximately 12% less BV in the first mm, the architectural arrangement shows a more rod-like and isotropic arrangement just beneath the SBP in OA in comparison to the plate-like and more anisotropic physiological arrangement. As stated above, the absolute differences decrease with depth and the logarithmic dependencies of the non-OA and OA samples show a narrowing of the curves toward the 5th mm. We cannot exclude a gain of material in initial stages of OA. In the advanced cases observed here, BV loss was always observed, and was most severe just below the mechanically altered SBP and is mostly due to a consequence of a reduced trabecular number (−23.20% in the first mm) than to the reduction of the trabecular thickness (−13.29% in the first mm).

The limitations of this study must be seen in the lack of knowledge of the medical-history of the body-donors concerning knee injuries as well as the limited number of samples. Furthermore we did not differentiate between male and female patellae. Merely the OA stage according to Outerbridge was of importance for sample collection. Although we compared OA patellae with non-OA patellae from a previous study, the methods used were exactly the same.

In conclusion, the data points to a decrease of OA activity with depth beneath the SBP and underlines the idea that the development of the disease starts well above the SBP and trabecular network and progress downwards. Future studies on cell level will have to determine the reasons of differences in bone turnover in the consecutive mms within the trabecular system and aim to explain the cell-mechanisms behind.

AUTHORS' CONTRIBUTIONS

Sebastian Hoechel and Magdalena Müller-Gerbl designed the study. Sebastian Hoechel and Mireille Toranelli contributed to analysis and interpretation. Hans Deyhle committed to data acquisition and processing. Sebastian Hoechel drafted and finalized the paper. All authors have read and approved of the final manuscript.

REFERENCES

1. Simkin PA, Graney DO, Fiechtner JJ. 1980. Roman arches, human joints, and disease. Arthritis Rheum 23:1308–1311.
2. Simkin PA, Heston TF, Downey DJ, et al. 1991. Subchondral architecture in bones of the canine shoulder. J Anat 175:213.
3. Clark JM, Huber JD. 1990. The structure of the human subchondral plate. J Bone Joint Surg Br 72:866–873.
4. Milz S, Eckstein F, Putz R. 1997. Thickness distribution of the subchondral mineralization zone of the trochlear notch and its correlation with the cartilage thickness: an expression of functional adaptation to mechanical stress acting on the humeroulnar joint? Anat Rec 248:189–197.
5. Milz S, Putz R. 1994. Quantitative morphology of the subchondral plate of the tibial plateau. J Anat 185:103–110.
6. Muller-Gerbl M. 1998. The subchondral bone plate. Adv Anat Embryol Cell Biol 141:1–134.
7. Zumstein V, Kraljević M, Müller-Gerbl M. 2013. Glenohumeral relationships: subchondral mineralization patterns, thickness of cartilage, and radii of curvature. J Orthop Res 31:1704–1707.
8. Leumann A, Valderrabano V, Hoechel S, et al. 2015. Mineral density and penetration strength of the subchondral bone plate of the talar dome: high correlation and specific distribution patterns. J Foot Ankle Surg 54:17–22.
9. Eckstein F, Muller-Gerbl M, Putz R. 1992. Distribution of subchondral bone density and cartilage thickness in the human patella. J Anat 180:425–433.
10. Anetzberger H, Mayer A, Glaser C, et al. 2014. Meniscectomy leads to early changes in the mineralization distribution of subchondral bone plate. Knee Surg Sports Traumatol Arthrosc 22:112–119.
11. Wolff J. 1986. The law of bone remodeling [translated from the 1892 original, Das Gesetz der Transformation der Knochen, by P. Maquet and R. Furlong]. Berlin: Springer Verlag.
12. Ding M, Odgaard A, Hvid I. 1999. Accuracy of cancellous bone volume fraction measured by micro-CT scanning. J Biomech 32:323–326.
13. Hildebrand T, Laib A, Müller R, et al. 1999. Direct three-dimensional morphometric analysis of human cancellous bone: microstructural data from spine, femur, iliac crest, and calcaneus. J Bone Miner Res 14:1167–1174.
14. Hildebrand T, Rüegsegger P. 1997. A new method for the model-independent assessment of thickness in three-dimensional images. J Microsc 185:67–75.
15. Evans FG, King AI. 1961. Regional differences in some physical properties of human spongy bone. Biomechanical studies of the musculo-skeletal system. IL: Charles C Thomas Springfield. p 19–67.
16. Goldstein SA. 1987. The mechanical properties of trabecular bone: dependence on anatomic location and function. J Biomech 20:1055–1061.
17. Hoechel S, Schulz G, Müller-Gerbl M. 2015. Insight into the 3D-trabecular architecture of the human patella. Ann Anat 200:98–104.
18. Nowakowski AM, Deyhle H, Zander S, et al. 2013. Micro CT analysis of the subarticular bone structure in the area of the talar trochlea. Surg Radiol Anat 35: 283–293.
19. Sun HB. 2010. Mechanical loading, cartilage degradation, and arthritis. Ann NY Acad Sci 1211:37–50.
20. Valderrabano V, Horisberger M, Russell I, et al. 2009. Etiology of ankle osteoarthritis. Clin Orthop Relat Res 467:1800–1806.
21. Tecklenburg K, Dejour D, Hoser C, et al. 2006. Bony and cartilaginous anatomy of the patellofemoral joint. Knee Surg Sports Traumatol Arthrosc 14:235–240.
22. Madry H, van Dijk CN, Mueller-Gerbl M. 2010. The basic science of the subchondral bone. Knee Surg Sports Traumatol Arthrosc 18:419–433.
23. Radin EL, Parker HG, Pugh JW, et al. 1973. Response of joints to impact loading—III: relationship between trabecular microfractures and cartilage degeneration. J Biomech 6:51–57.
24. Burr DB, Martin RB, Schaffler MB, et al. 1985. Bone remodeling in response to in vivo fatigue microdamage. J Biomech 18:189–200.
25. Sharma L, Kapoor D. 2007. Epidemiology of osteoarthritis. Osteoarthritis: diagnosis and medical/surgical management. Philadelphia: PA Saunders. p 3.
26. Guccione AA, Felson DT, Anderson JJ, et al. 1994. The effects of specific medical conditions on the functional limitations of elders in the Framingham study. Am J Public Health 84:351–358.

27. Neuman P, Kostogiannis I, Fridén T, et al. 2009. Patellofemoral osteoarthritis 15 years after anterior cruciate ligament injury—a prospective cohort study. Osteoarthritis Cartilage 17:284–290.
28. Englund M, Lohmander L. 2005. Patellofemoral osteoarthritis coexistent with tibiofemoral osteoarthritis in a meniscectomy population. Ann Rheum Dis 64:1721–1726.
29. Iriuchishima T, Ryu K, Aizawa S, et al. 2012. Evaluation of the prevalence, lesion, and depth of osteoarthritic changes in the patella. Knee Surg Sports Traumatol Arthrosc 20:2460–2464.
30. Ding M. 2010. Microarchitectural adaptations in aging and osteoarthrotic subchondral bone issues. Acta Orthop Suppl 81:1–53.
31. Hannan MT, Anderson JJ, Zhang Y, et al. 1993. Bone mineral density and knee osteoarthritis in elderly men and women. The Framingham study. Arthritis Rheum 36:1671–1680.
32. Muller-Gerbl M, Putz R, Hodapp N, et al. 1989. Computed tomography-osteoabsorptiometry for assessing the density distribution of subchondral bone as a measure of long-term mechanical adaptation in individual joints. Skeletal Radiol 18:507–512.
33. Feldkamp L, Davis L, Kress J. 1984. Practical cone-beam algorithm. JOSA A 1:612–619.
34. Dempster DW, Compston JE, Drezner MK, et al. 2013. Standardized nomenclature, symbols, and units for bone histomorphometry: a 2012 update of the report of the ASBMR Histomorphometry Nomenclature Committee. J Bone Miner Res 28:2–17.
35. Hildebrand T, Ruegsegger P. 1997. Quantification of bone microarchitecture with the structure model index. Comput Methods Biomech Biomed Engin 1:15–23.
36. Parfitt AM, Drezner MK, Glorieux FH, et al. 1987. Bone histomorphometry: standardization of nomenclature, symbols, and units: report of the ASBMR Histomorphometry Nomenclature Committee. J Bone Miner Res 2:595–610.
37. Ficat RP, Hungerford DS. 1977. Disorders of the patellofemoral joint. Baltimore: Williams & Wilkins.
38. Hoechel S, Wirz D, Muller-Gerbl M. 2012. Density and strength distribution in the human subchondral bone plate of the patella. Int Orthop 36:1827–1834.
39. Muller-Gerbl M, Weisser S, Linsenmeier U. 2008. The distribution of mineral density in the cervical vertebral endplates. Eur Spine J 17:432–438.
40. Burr DB, Gallant MA. 2012. Bone remodelling in osteoarthritis. Nat Rev Rheumatol 8:665–673.
41. Henrotin Y, Pesesse L, Sanchez C. 2012. Subchondral bone and osteoarthritis: biological and cellular aspects. Osteoporos Int 23:847–851.
42. Thambyah A, Broom N. 2009. On new bone formation in the pre-osteoarthritic joint. Osteoarthritis Cartilage 17:456–463.
43. Suri S, Walsh DA. 2012. Osteochondral alterations in osteoarthritis. Bone 51:204–211.
44. Lories RJ, Luyten FP. 2011. The bone-cartilage unit in osteoarthritis. Nat Rev Rheumatol 7:43–49.
45. Patel V, Issever AS, Burghardt A, et al. 2003. MicroCT evaluation of normal and osteoarthritic bone structure in human knee specimens. J Orthop Res 21:6–13.
46. Dedrick, D.K., Goldstein SA, Brandt KD, et al., 1993. A longitudinal study of subchondral plate and trabecular bone in cruciate-deficient dogs with osteoarthritis followed up for 54 months.
47. Ding M, Hvid I. 2000. Quantification of age-related changes in the structure model type and trabecular thickness of human tibial cancellous bone. Bone 26:291–295.
48. Florea C, Malo MKH, Rautiainen J, et al. 2015. Alterations in subchondral bone plate, trabecular bone and articular cartilage properties of rabbit femoral condyles at 4 weeks after anterior cruciate ligament transection. Osteoarthritis Cartilage 23:414–422.
49. Kamibayashi L, Wyss UP, Cooke TDV, et al. 1995. Trabecular microstructure in the medial condyle of the proximal tibia of patients with knee osteoarthritis. Bone 17:27–35.
50. Buckland-Wright J, Lynch J, Macfarlane D. 1996. Fractal signature analysis measures cancellous bone organisation in macroradiographs of patients with knee osteoarthritis. Ann Rheum Dis 55:749–755.